Development 134, 1737-1744 (2007) doi:10.1242/dev.02831

grp (*chk1*) replication-checkpoint mutations and DNA damage trigger a Chk2-dependent block at the *Drosophila* midblastula transition

Saeko Takada*, Seongae Kwak, Birgit S. Koppetsch and William E. Theurkauf†

The 13 syncytial cleavage divisions that initiate *Drosophila* embryogenesis are under maternal genetic control. The switch to zygotic regulation of development at the midblastula transition (MBT) follows mitosis 13, when the cleavage divisions terminate, transcription increases and the blastoderm cellularizes. Embryos mutant for *grp*, which encodes Checkpoint kinase 1 (Chk1), are DNA-replication-checkpoint defective and fail to cellularize, gastrulate or to initiate high-level zygotic transcription at the MBT. The *mnk* (also known as *loki*) gene encodes Checkpoint kinase 2 (Chk2), which functions in DNA-damage signal transduction. We show that *mnk grp* double-mutant embryos are replication-checkpoint defective but cellularize, gastrulate and activate high levels of zygotic gene expression. We also show that *grp* mutant embryos accumulate DNA double-strand breaks and that DNA-damaging agents induce a *mnk*-dependent block to cellularization and zygotic gene expression. We conclude that the DNA-replication checkpoint maintains genome integrity during the cleavage divisions, and that checkpoint mutations lead to DNA damage that induces a novel Chk2-dependent block at the MBT.

KEY WORDS: DNA damage, MBT, Transcription, Cellularization, *Drosophila*

INTRODUCTION

In most metazoans, embryogenesis is initiated by a series of rapid mitotic divisions that are driven by mRNAs and proteins that accumulate during oogenesis (Foe et al., 1993). The cleavage stage is therefore under maternal genetic control. Embryonic development first requires zygotic gene expression at the midblastula transition (MBT), when the cell cycle slows, gene transcription increases dramatically and a subset of maternal mRNAs are degraded (O'Farrell et al., 2004). There is no growth during the cleavage stage, and the rapid cleavage-stage mitoses thus lead to progressive increases in the ratio of nuclei to cytoplasm (nucleocytoplasmic ratio). Reducing the number of nuclei or DNA content during the cleavage stage leads to additional mitotic divisions prior to the MBT, whereas increasing the DNA content reduces the number of pre-MBT divisions (Edgar et al., 1986; Kane and Kimmel, 1993; Newport and Kirschner, 1982). These observations suggest that titration of a maternally deposited factor by nuclear components triggers the MBT (Newport and Kirschner, 1982). However, the titrated maternal factor has not been identified, and some aspects of the MBT are controlled by a developmental timer that is independent of the cleavage divisions (Bashirullah et al., 1999; Hartley et al., 1996; Hartley et al., 1997). The molecular mechanisms that control the MBT thus remain to be defined.

In *Drosophila*, the maternally controlled cleavage-stage divisions are syncytial and zygotic control of development begins as the blastoderm cellularizes (Foe et al., 1993). Mutations in the genes *grp* and *mei-41*, which, respectively, encode the kinases Chk1 and Atr, which are required for the DNA-replication checkpoint, block cellularization and high-level zygotic gene activation at the *Drosophila* MBT. The cleavage-stage cell cycle progressively slows during syncytial blastoderm divisions 10 through to 13, but embryos mutant for *grp* or *mei-41* fail to slow the syncytial blastoderm cell cycle and proceed through extra cleavage-stage cycles (Sibon et al., 1999; Sibon et al., 1997). These observations support a model in which maternal DNA-replication factors are titrated during the late syncytial divisions, leading to increases in S-phase length that trigger replication-checkpoint-dependent delays in progression into mitosis (Sibon et al., 1999; Sibon et al., 1997). However, the relationship between checkpoint-dependent cell cycle delays during the late syncytial divisions and the defects in zygotic gene activation and cellularization at the MBT have not been established.

Chk2 is a conserved kinase that functions in DNA-damage signaling. Here, we show that mutations in the *mnk* (also known as *loki* – FlyBase) gene, which encodes Chk2, suppress the cellularization, gastrulation and zygotic gene-activation defects associated with *grp* mutations. However, *mnk grp* double-mutant embryos lack a functional replication checkpoint and do not show wild-type cleavage-stage cell cycle delays. Progression through the MBT does therefore not require normal increases in cell cycle length during the late cleavage stage, or require Chk1. We also show that *grp* mutant embryos accumulate DNA double-strand breaks, and that DNA-damaging agents block zygotic gene activation and cellularization in wild-type embryos, but not in *mnk* mutants. These findings indicate that the crucial developmental function for the replication checkpoint is to maintain genome integrity during the rapid cleavage-stage divisions, and that checkpoint mutations block to the MBT by activating a novel Chk2-dependent pathway that inhibits cellularization and zygotic gene expression.

MATERIALS AND METHODS

Drosophila stocks

The grp^{fs1} and mnk^{P6} alleles are protein nulls (Brodsky et al., 2004; Sibon et al., 1997) (data not shown). w^{1118} was used as a control because both mutant alleles are in the w^{1118} background. To obtain grp^{fs1} and mnk^{P6} grp^{fs1}

Program in Molecular Medicine, Program in Cell Dynamics, University of Massachusetts Medical School, 373 Plantation Street, Worcester, MA 01605, USA.

*Present address: Washington University School of Medicine, Department of Cell Biology and Physiology, 660 S. Euclid Avenue, St Louis, MO 63110, USA
†Author for correspondence (e-mail: william.theurkauf@umassmed.edu)

Accepted 12 February 2007

double-mutant embryos, homozygous females were mated to wild-type (Oregon R) males. To obtain *mnk*^{P6} mutant embryos, homozygous-mutant females were mated to homozygous-mutant males.

Immunofluorescence

At 2-3 hours of age, embryos were fixed with formaldehyde/methanol and immunostained with mouse anti-α-Spectrin monoclonal antibody 3A9 (1:10 dilution, Developmental Studies Hybridoma Bank) as described (Theurkauf, 1994). DNA was stained with 0.2 μM TOTO3 (Molecular Probes). To cytologically assay for DNA double-strand breaks, 1-3-hour-old *grp* embryos were fixed with methanol and immunostained with rabbit anti-phospho-Histone H2.A.X (Ser139) (γH2AX) antibody (1:250 dilution, Upstate) as described (Theurkauf, 1994). The embryos were imaged using a Leica TCS-SP inverted scanning confocal microscope. ImageJ was used for image processing (Rasband, W.S., ImageJ, U.S. National Institutes of Health, Bethesda, Maryland, USA, http://rsb.info.nih.gov/ij/, 1997-2006).

DNA-damage treatment and whole-mount in situ hybridization

To induce DNA damage, wild-type (w^{1118}) or *mnk* mutant embryos were bleach dechorionated, rinsed with Triton/NaCl and H_2O, and treated in a 1:1 mixture of octane and Robb's medium (55 mM potassium acetate, 40 mM sodium acetate, 100 mM sucrose, 10 mM glucose, 1.2 mM $MgCl_2$, 1 mM $CaCl_2$ and 100 mM HEPES, pH 7.4) containing 50 μg/ml bleomycin (Sigma) for 30 minutes. To assay transcription, embryos were then fixed in methanol (Theurkauf, 1994), rehydrated and processed for enhanced fluorescence in situ hybridization. Anti-sense digoxigenin (DIG)-labeled RNA probes were synthesized from cDNA clones or PCR-amplified cDNA fragments using DIG-High Prime following the manufacturer's instructions (Roche). *runt* and *fushi tarazu* cDNA clones were provided by P. Gergen (Tsai and Gergen, 1995). *slam* (*slow as molasses*) and *sry-α* DNA fragments were amplified by PCR using wild-type genomic DNA and gene-specific primers [for *slam*, 5′-CTGTTCAGTCCGATTCTC-3′ and 5′-CGTAA-TACGACTCACTATAGGG-3′ (T7 promoter sequence)+5′-AATCTTGTC-CATGTGCTCGCTG-3′; for *sry-α*, 5′-CTCTGACCACTTGGATGACTA-3′ and 5′-CGTAATACGACTCACTATAGGG-3′ (T7)+5′-GATTCAGCAA-GTGAGTCCTGTG-3′]. Whole-mount in situ hybridization was performed as described (Tautz and Pfeifle, 1989; Cha et al., 2001). Tyramide signal amplification (TSA) was performed following manufacturer's instructions (Perkin Elmer). Briefly, after the post-hybridization washes, embryos were blocked for 30 minutes in TNB buffer [0.1 M Tris-HCl (pH 7.5), 0.15 M NaCl, 0.5% block-TSA kit], incubated for 2 hours at room temperature with anti-Digoxigenin POD (Roche) at 1:100 dilution in TNB and washed three times, for 5 minutes each, in PBST (1×PBS, 0.05% Triton X-100). Embryos were then incubated for 20 minutes with fluorophore tyramide, 1 μg/ml RNase ONE (Promega) and 0.2 μM TOTO3 (Molecular Probes), washed three times, for 5 minutes each, with PBST, and mounted in PBS/glycerol containing p-phenylenediamine dihydrochloride (9:1 glycerol:10×PBS, 1 mg/ml p-phenylenediamine dihydrochloride) (Sigma). The embryos were imaged using a Leica TCS-SP inverted scanning confocal microscope. Identical probes, in situ hybridization procedures and imaging conditions were used for all embryos.

Live-embryo imaging

For live analysis of the syncytial blastoderm stage, 0-2-hour-old embryos were manually dechorionated, placed on a cover glass and covered with halocarbon oil (Sigma) (Sibon et al., 1997). Differential interference contrast (DIC) images were captured on a Zeiss Axiovert S100 inverted microscope equipped with a Uniblitz VMM-D1 (Vincent Associate) computer-operated shutter and a Coolsnap HQ CCD camera (Photometrics). MetaMorph software (Universal Imaging) was used for recording and image processing. Images were captured with 50 millisecond exposure at 20 second intervals. Cell cycle timing was calculated by counting the number of frames between nuclear-envelope formation and breakdown. To induce DNA damage, bleomycin (Sigma) at 50 μg/ml and rhodamine-conjugated tubulin (Cytoskeleton) at 5 mg/ml were co-injected into syncytial embryos. The embryos were imaged using a Leica TCS-SP inverted scanning confocal microscope. Cell cycle number and phase were determined from nuclear density and microtubule organization (Sibon et al., 1997).

Antibodies and western blotting

Rabbit Chk2C antibodies were raised against a keyhole limpet hemocyanin-conjugated C-terminal peptide of *Drosophila* Chk2 (Mnk) [(C)NFLEPPTKRSRR] (Invitrogen) and affinity-purified using oligopeptide coupled to SulfoLink Coupling Gel following the manufacturer's instructions (Pierce). Rabbit anti-Phospho-cdc2 (Tyr15) antibody and mouse anti-α-Tubulin monoclonal antibody (B-5-1-2) were purchased from Cell Signaling and Sigma, respectively. Donkey anti-rabbit IgG and anti-mouse IgG antibodies conjugated with peroxidase were purchased from Amersham. For western blot analysis, embryos were collected on grape juice agar plates, aged after deposition as indicated (0-1, 1-2, 2-3, 3-4 hours), lysed in SDS-PAGE sample buffer, boiled for 5 minutes and loaded on either 18×20 cm 8.5% polyacrylamide gels (for Chk2) or 8×8 cm 12% polyacrylamide gels (for phospho-Cdc2). Proteins were then transferred onto Hybond-C Extra membrane (Amersham) and western blotting was performed with standard procedures. Briefly, the membrane was blocked in 5% non-fat milk/Tween-TBS (0.02% Tween, 1×TBS) overnight at 4°C, incubated with primary antibodies for 2 hours at room temperature, washed with Tween-TBS, incubated with secondary antibodies for 30 minutes and washed with Tween-TBS. The membranes were detected with an ECL Plus western blotting detection system (Amersham).

RESULTS

mnk suppresses *grp* arrest at the MBT

For all of the following studies, we assayed embryos derived from homozygous single- and double-mutant females that were mated to wild-type males. These embryos were therefore heterozygous for the mutation(s) under investigation. Early embryogenesis is, however, under maternal genetic control; we therefore refer to these embryos by the maternal genotype here.

Embryos mutant for *grp*, which encodes an essential component of the DNA-replication checkpoint, arrest development at the MBT (Sibon et al., 2000; Sibon et al., 1997). The *grp* mutation also causes spindle-assembly defects during the late syncytial divisions (Sibon et al., 2000), and these mitotic defects are suppressed by a null mutation in *mnk* (Takada et al., 2003), which encodes a Chk2 homolog required for DNA-damage signaling (Bartek et al., 2001; Brodsky et al., 2004; Masrouha et al., 2003; Peters et al., 2002). To determine whether the MBT block in *grp* mutants also requires Chk2, we analyzed the development of embryos that lack maternal Chk1 and Chk2. Embryos double-mutant for *mnk* and *grp* (*mnk grp*), like *grp* single mutants, failed to hatch. The *mnk* mutation thus does not suppress the maternal-effect embryonic lethality associated with *grp*.

To determine whether *mnk* suppresses the developmental block at the MBT, embryos were assayed for cellularization, which is the first morphogenetic event that requires zygotic gene expression (Postner and Wieschaus, 1994; Schejter and Wieschaus, 1993; Wieschaus and Sweeton, 1988). During cellularization, the monolayer of cortical nuclei is surrounded by a characteristic hexagonal array of membranes with associated actin filaments. This arrangement is clearly observed in wild-type and *mnk* mutant embryos (Fig. 1A,B). In similarly aged *grp* mutants, by contrast, the syncytial nuclei are randomly distributed and the actin network, detected with an antibody to α-Spectrin, is highly disorganized (Sibon et al., 2000) (Fig. 1C, *grp*). These studies, and extensive previous observations, indicate that 100% of *grp*-null mutant embryos fail to cellularize. Strikingly, a significant number of *mnk grp* double-mutant embryos had a uniform monolayer of cortical nuclei surrounded by a hexagonal actin network, indicating that they had initiated or completed cellularization (Fig. 1D, *mnk grp*). The nuclei in the double-mutant embryos were larger than in wild-type controls (Fig. 1D, inset), and this appears to result from chromosome-segregation

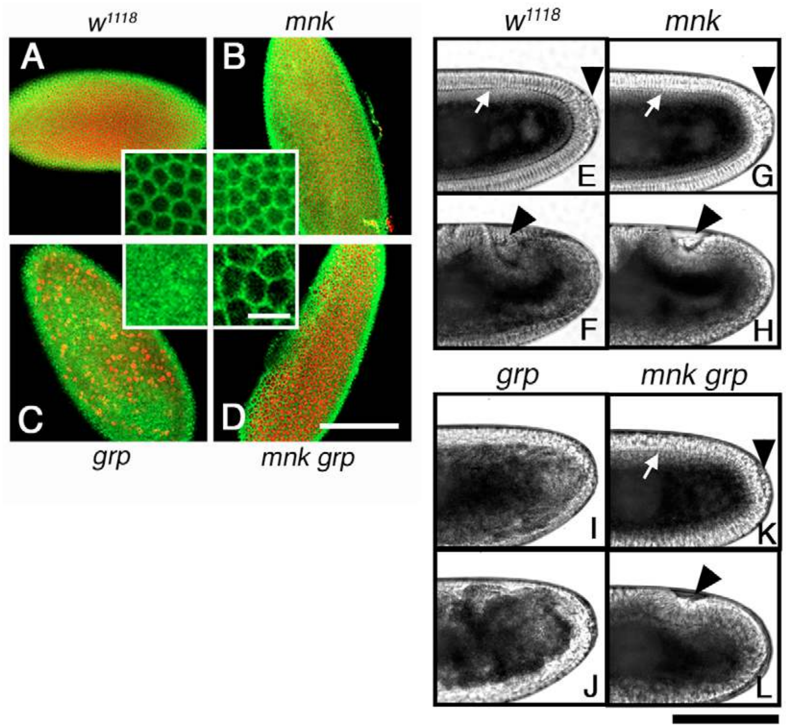

Fig. 1. An *mnk*-null mutation suppresses the cellularization- and gastrulation-defects associated with the *grp* mutation. (**A**,**B**) Control (w^{1118}) and *mnk*-null mutant (*mnk*) embryos cellularize during interphase 14; a uniform monolayer of nuclei surrounded by a hexagonal network of membrane and associated actin network (insets) can be seen. (**C**) *grp*-null mutant embryos fail to cellularize and nuclei are either lost from the surface or fuse to form aggregates, and the actin cytoskeleton is disorganized (inset). (**D**) By contrast, *mnk grp* double-mutant embryos cellularize and show a near wild-type hexagonal actin network and uniform cortical nuclear monolayer (inset). However, the nuclei are significantly larger than in wild-type or *mnk* mutant embryos. (A-D) The actin cytoskeleton (green) was labeled with an anti-α-Spectrin antibody and nuclei were labeled with TOTO3 (Molecular Probes; red). Insets are enlarged images of α-Spectrin staining. (**E-L**) Still images from transmitted light time-lapse recordings of control (w^{1118}), *mnk*- and *grp*-null single mutant, and *mnk grp* double-mutant embryos. Control (E,F), *mnk*-null mutant (G,H) and *mnk grp* double-mutant (K,L) embryos cellularize and gastrulate. By contrast, *grp*-null mutant embryos (I,J) do not cellularize or gastrulate. Arrows indicate the cellularization front; arrowheads indicate pole cells migrating towards the anterior during gastrulation. Scale bars: 100 μm in A-L; 10 μm in insets in A-D.

failures during the late syncytial blastoderm divisions (Takada et al., 2003). These initial observations indicated that the *mnk* mutation at least partially suppresses the cellularization/MBT block associated with the *grp* mutation.

To evaluate how efficiently *mnk* suppresses the cellularization defects associated with the *grp* mutation, we directly analyzed early embryogenesis by time-lapse transmitted light microscopy. In wild-type (w^{1118}) and *mnk* mutant embryos, cellularization consistently takes place after mitosis 13, when the cell cycle pauses and membrane invaginations surround the cortical nuclei. Completion of cellularization is immediately followed by the morphogenetic movements of gastrulation, which include anterior migration of pole cells (germline cells) (Fig. 1E-H, and see Movies 1, 2 in the supplementary material). All of the *grp* mutants examined (100%; n=20) exited mitosis 13 and immediately continued through additional cleavage cycles. These embryos never cellularized and became increasingly disorganized during these additional cleavage cycles (Sibon et al., 1997) (Fig. 1I,J, and see Movie 3 in the supplementary material). By contrast, nine out of nine *mnk grp* double-mutant embryos analyzed by time-lapse microscopy cellularized and gastrulated (Fig. 1K,L, and see Movie 4 in the supplementary material). The cephalic furrow, which normally forms as pole-cell movement is initiated, did not form in *mnk grp* double mutants (see Movies 1, 2, 4 in the supplementary material). The *mnk grp* embryos also consistently proceeded through a fifth cortical mitotic cycle (14th cycle)

Table 1. Pre-MBT cell cycle timing and duration from pole-cell migration to cellularization in wild-type and mutant embryos

Cell cycle timing*

Cell cycle	Wild type (6)	*mnk* (*chk2*) (5)	*grp* (*chk1*) (5)	*mnk grp* (9)
10 I	4.7±0.43	4.7±0.48	4.7±0.44	4.9±0.51
M	4.4±0.90	4.0±0.54	4.5±0.75	4.8±0.60
11 I	5.2±0.50	4.4±0.49	4.9±0.75	5.3±0.67
M	4.3±1.00	4.0±0.49	3.9±0.25	4.5±0.47
12 I	7.2±0.85	8.4±1.00	6.1±0.16	6.5±0.69
M	4.6±0.41	4.3±0.54	4.8±0.89	5.0±0.37
13 I	13.9±1.42	15.9±2.24	7.1±0.83	9.7±0.93
M	4.8±0.54	5.0±0.83	8.1±0.80	4.9±0.71
14 I	NA	NA	10.9±0.62	12.6±1.20
M	NA	NA	13.8±1.38	6.7±0.89

Pole-cell migration to cellularization**

	Wild type	*mnk* (*chk2*)	*grp* (*chk1*)	*mnk grp*
Int	71.0±2.89 (6)	68.9±2.42 (5)	NA	83.5±3.15 (8)
Mid	104.6±5.15 (6)	102.3±4.05 (5)	NA	125.7±6.10 (6)

*Average durations±s.d. of cell cycle timing are shown. Timing of nuclear envelope formation (NEF) and nuclear envelope breakdown (NEB) were measured from DIC live recordings of embryos. I, interphase from NEF to NEB; M, mitosis from NEB to NEF. Number of embryos analyzed are shown in parentheses.
**Average durations±s.d. from pole-cell migration (pole-bud formation) to cellularization are shown. Number of embryos analyzed are shown in parentheses. Int, initiation of membrane invagination; Mid, invaginating membrane reaches to approximately one third of the final cell length; NA, not analyzed.

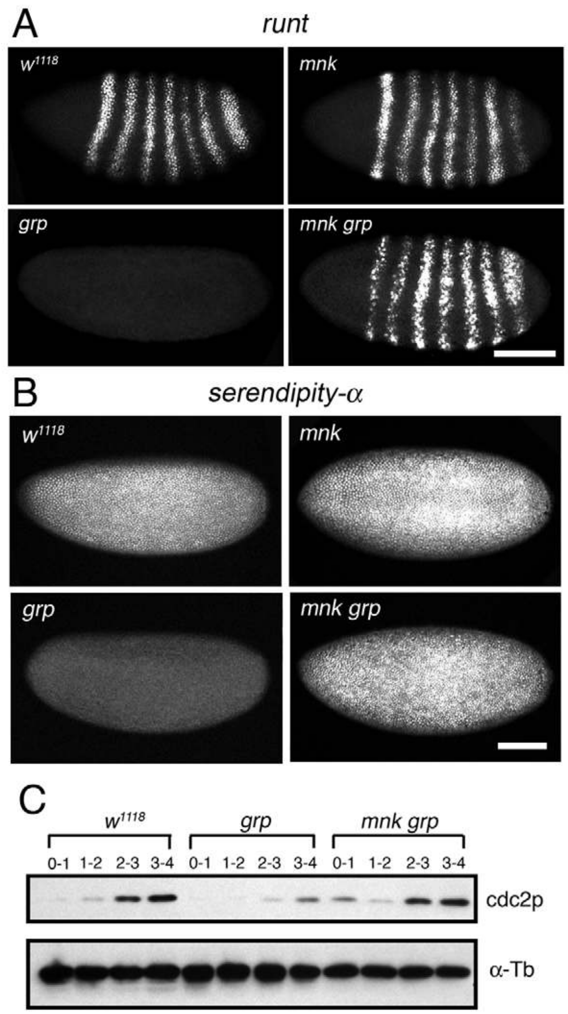

Fig. 2. The *mnk* mutation suppresses zygotic gene transcription and Cdc2-phosphorylation defects in *grp* mutant embryos. (**A**,**B**) Whole-mount in situ hybridization of the segmentation gene *runt* (A) and the cellularization gene *serendipity-α* (B). (A) Control (w^{1118}) and *mnk*-null mutant embryos show seven-stripe *runt* transcript expression during interphase 14. The *runt* gene is never expressed at high levels in *grp*-null mutant embryos. By contrast, seven-stripe *runt* expression is clearly observed in *mnk grp* double-null mutant embryos. (B) *serendipity-α* is required for cellularization and is expressed at high levels during interphase 14 in both wild-type (w^{1118}) and *mnk* mutant embryos, but not in *grp* mutant embryos. Expression of *serendipity-α* is also restored in *mnk grp* double mutants. (**C**) In control (w^{1118}) and *mnk* mutants, inhibitory tyrosine phosphorylation of Cdc2 dramatically increases at the MBT, between 2 and 4 hours post-egg-deposition. This dramatic increase in Cdc2 phosphorylation is not observed in *grp* mutant embryos. In *mnk grp* double-mutant embryos, however, essentially wild-type Cdc2 phosphorylation is restored (at 2-3 and 3-4 hours). Western blots of embryonic lysates were probed with antibodies against phospho-Cdc2 (Tyrosine 15), and α-Tubulin was used as the loading control. Embryo age in hours is indicated (0-1,1-2, 2-3 and 3-4). Scale bars: 100 μm.

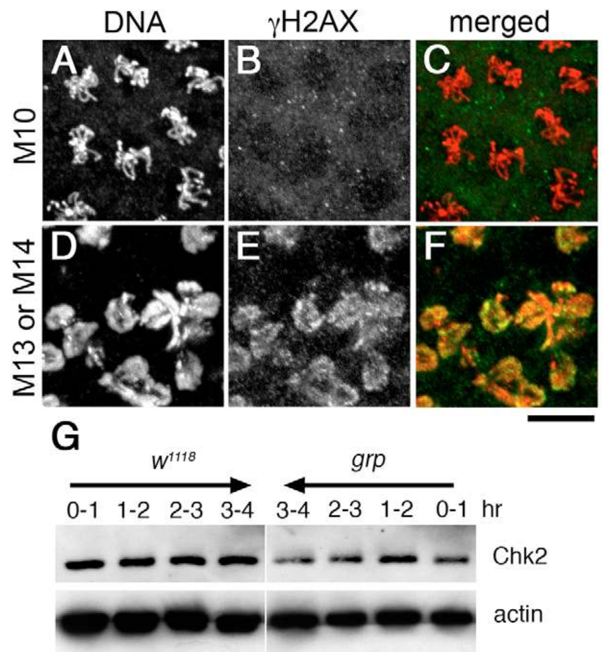

Fig. 3. DNA double-strand-break accumulation in *grp* mutant embryos. (**A-F**) To assay for DNA damage in *grp* mutants, embryos were stained with an antibody that recognizes a phosphorylated form of histone H2AX (*Drosophila* homolog: Histone H2Av) (anti-γH2AX), and for DNA with TOTO3. (A-C) γH2AX labeling is not observed in early *grp* mutant embryos. (D-F) However, γH2AX labeling becomes prominent in *grp* mutant embryos after mitosis 13. Cellularization consistently fails in these mutants (Sibon et al., 1997). (C,F) DNA, red; phospho-histone-H2Av, green. (**G**) Chk2 phosphorylation in *grp* mutant embryos. Extracts from developmentally staged wild-type (w^{1118}) and *grp* mutant embryos were assayed for Chk2 expression by western blotting. Chk2 shows reduced electrophoretic mobility, characteristic of activating phosphorylation, in 3-4 hour *grp* mutants, but not in wild-type controls. Scale bar: 10 μm.

before cellularization (see Movie 4 in the supplementary material), and chromosome segregation failed during the later syncytial divisions, producing polyploid nuclei (Takada et al., 2003). The polyploidy resulting from division failures during the late cleavage stage may contribute to the gastrulation defects and embryonic lethality in the double mutants. Nonetheless, the *mnk* mutation dramatically suppressed the developmental arrest associated with the *grp* mutation, allowing consistent cellularization and gastrulation.

We previously speculated that *grp* mutants fail to progress through the MBT because the shortened syncytial blastoderm cell cycle times do not allow complete transcription of early zygotic genes (Sibon et al., 1997). However, the cell cycle times in *mnk grp* double mutants are significantly shorter than in wild type, yet these double mutants cellularize (Table 1). In addition, zygotic expression of a number of genes, including *slam* and *serendipity-α* (*sry-α*), peak very early in interphase 14, at or before the start of cellularization, which is initiated 10 minutes after the completion of mitosis 13 (Foe et al., 1993) (see Movie 1 in the supplementary material). Zygotic gene activation thus requires significantly less than 10 minutes, and interphase 14 in *grp* mutants averages 11-12 minutes (Sibon et al., 1999; Sibon et al., 1997) (Table 1). The cell cycle timing defects in *grp* mutants are therefore insufficient to account for the observed block in cellularization and gene expression.

These observations, however, do not eliminate the possibility that signaling through the replication checkpoint is required for transcription and cellularization, and that the *mnk* mutations restore this signaling. To directly test for replication-checkpoint function in *mnk grp* double mutants, we co-injected embryos with the DNA-polymerase inhibitor aphidicolin and with rhodamine-conjugated tubulin, and analyzed progression into mitosis 11 and 12 by time-lapse confocal microscopy (Sibon et al., 1997). In wild-type embryos, aphidicolin induced an increase in interphase length from 5.4 minutes (s.d. 0.46, n=8) to 14.2 minutes (s.d. 1.5, n=8). By contrast, interphase length in *mnk grp* double mutants was 4.6 minutes (s.d. 2.7, n=8) under control conditions and 4.9 minutes (s.d. 0.21, n=6) following aphidicolin injection. Therefore, in the absence of Chk2, cellularization does not require a functional replication checkpoint or wild-type cell cycle delays during the syncytial blastoderm stage.

Cellularization is coordinated with a dramatic increase in inhibitory phosphorylation of the mitotic Cdc2 kinase (Edgar et al., 1994). The *grp* mutation blocks the increase in Cdc2 phosphorylation that normally accompanies interphase 14 and cellularization, and the Chk1 encoded by *grp* inhibits Cdc25, a dual specificity phosphatase that activates Cdc2 by reversing this modification (Walworth, 2001). These findings suggest that Chk1 activation leads to increases in Cdc2 phosphorylation during interphase 14, and that this modification may be essential to cellularization (Sibon et al., 1997). We therefore assayed *mnk grp* double-mutant embryos, which lack Chk1, for Cdc2 phosphorylation. As shown in Fig. 2C, Cdc2 phosphorylation is restored in *mnk grp* mutants, indicating that this process does not require Chk1 or a functional replication checkpoint. Maternal Cdc25 mRNA and protein, which are encoded by *string* and *twine*, are normally degraded early in interphase 14, and these processes require zygotic gene expression (Edgar and Datar, 1996; Edgar et al., 1994). The *grp* mutation could therefore inhibit Cdc2 phosphorylation by activating a Chk2-dependent block to the expression of zygotic factors that trigger the destruction of maternal Cdc25 transcripts and proteins.

To determine whether *mnk* suppresses the transcriptional defects associated with *grp* mutations (Sibon et al., 1997), we assayed mutant embryos for the expression of the segmentation genes *runt* and *fushi tarazu* (*ftz*), and for two genes required for cellularization, *slam* and *sry-α* (Fig. 2A,B, and data not shown) (Lecuit et al., 2002; Schweisguth et al., 1990). Fluorescence in situ hybridization (FISH) revealed high-level expression of all four genes during interphase 14 in wild-type and *mnk* single-mutant embryos (Fig. 2A,B, w^{1118} and *mnk*). By contrast, *runt*, *ftz* (data not shown) and *sry-α* were not detectable in interphase 14 *grp* mutants (Fig. 2A,B, *grp*). The *slam* transcript was detected in *grp* mutants, although the mRNA was dispersed and expression appeared to be lower than in wild-type embryos (data not shown). Strikingly, essentially wild-type expression of all four genes was observed in *mnk grp* double-mutant embryos (Fig. 2A,B, *mnk grp*, and data not shown). Chk2 is therefore required for the block to zygotic gene activation in *grp* mutants.

Mutations in the *grp* locus have been reported to stabilize Cyclin A and accelerate Histone H3 dephosphorylation on mitotic exit during the early cleavage divisions (Su et al., 1999). These defects could reflect a direct role for Chk1 during mitotic exit and in Cyclin A proteolysis, or result from checkpoint failure and Chk2 activation. In an attempt to distinguish between these alternatives, we analyzed Histone H3 dephosphorylation and Cyclin A protein levels in wild-type and mutant embryos. However, using standard immunocytological labeling, we found no significant difference in the kinetics of Histone H3 dephosphorylation in early cleavage-stage wild type or *grp* mutants (see Fig. S1 in the supplementary material). In addition, we found no significant difference in Cyclin A levels at

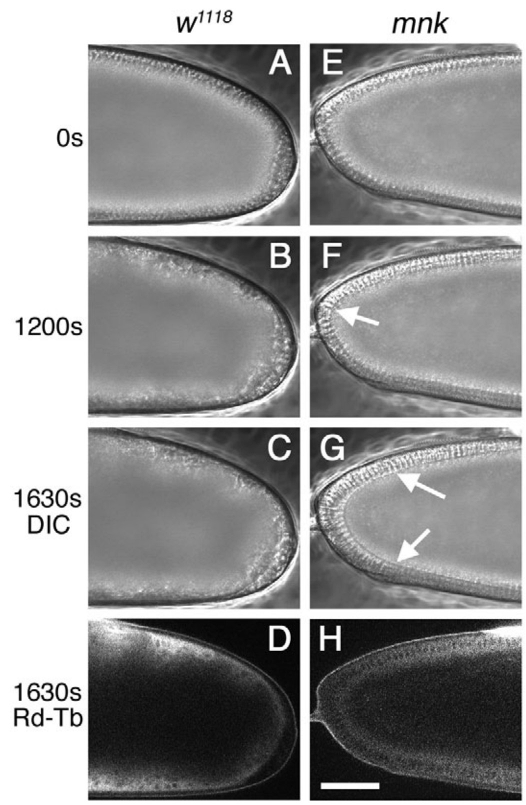

Fig. 4. DNA damage triggers a Chk2-dependent cellularization block. (**A-H**) Control (w^{1118}) and *mnk* mutant embryos were injected with bleomycin, and cellularization was monitored by time-lapse transmitted light and laser scanning confocal microscopy. Rhodamine-conjugated tubulin was co-injected as a marker for cell cycle stage. Nuclei exclude fluorescent rhodamine-conjugated tubulin and thus appear as dark circles on confocal imaging (Sibon et al., 1997). Recordings were started at the beginning of interphase 14 (0 seconds, 0s). Immediately after injection, nuclei were in a uniform monolayer in both wild-type (w^{1118}) and *mnk* mutant embryos (A,E). By 1200 seconds (1200s), the nuclear monolayer in w^{1118} controls was disorganized and some nuclei had dropped into the interior of the embryo (B), and these embryos did not cellularize (C,D). By contrast, all *mnk* mutant embryos injected with bleomycin consistently maintained a uniform nuclear monolayer and cellularized (E-H). (F,G) Plasma membrane invagination at the cellularization front is indicated (arrows). (D,H) Rhodamine-conjugated tubulin is excluded from interphase nuclei and was used as a cell cycle marker. (Also see Movies 1-5 in the supplementary material.) Scale bar: 50 μm.

0-90 minutes post-egg deposition in wild-type, *grp* or *mnk grp* embryos (see Fig. S2A in the supplementary material). We did see an increase in Cyclin A levels in 0-3-hour-old *grp* embryos (see Fig. S2B in the supplementary material), but this developmental pool included late syncytial blastoderm-stage embryos that were delayed in mitosis due to Chk2 activation (Table 1) (Takada et al., 2003). Significantly, 0-3-hour-old *mnk grp* double-mutant embryos did not overexpress Cyclin A (see Fig. S2B in the supplementary material). Increased Cyclin A accumulation in *grp* mutants thus appears to result from Chk2 activation. These findings, with the observations outlined above, indicate that the primary function of Chk1 is to delay cell cycle progression, thus preventing premature mitosis and DNA damage during the later syncytial blastoderm divisions. The mitotic

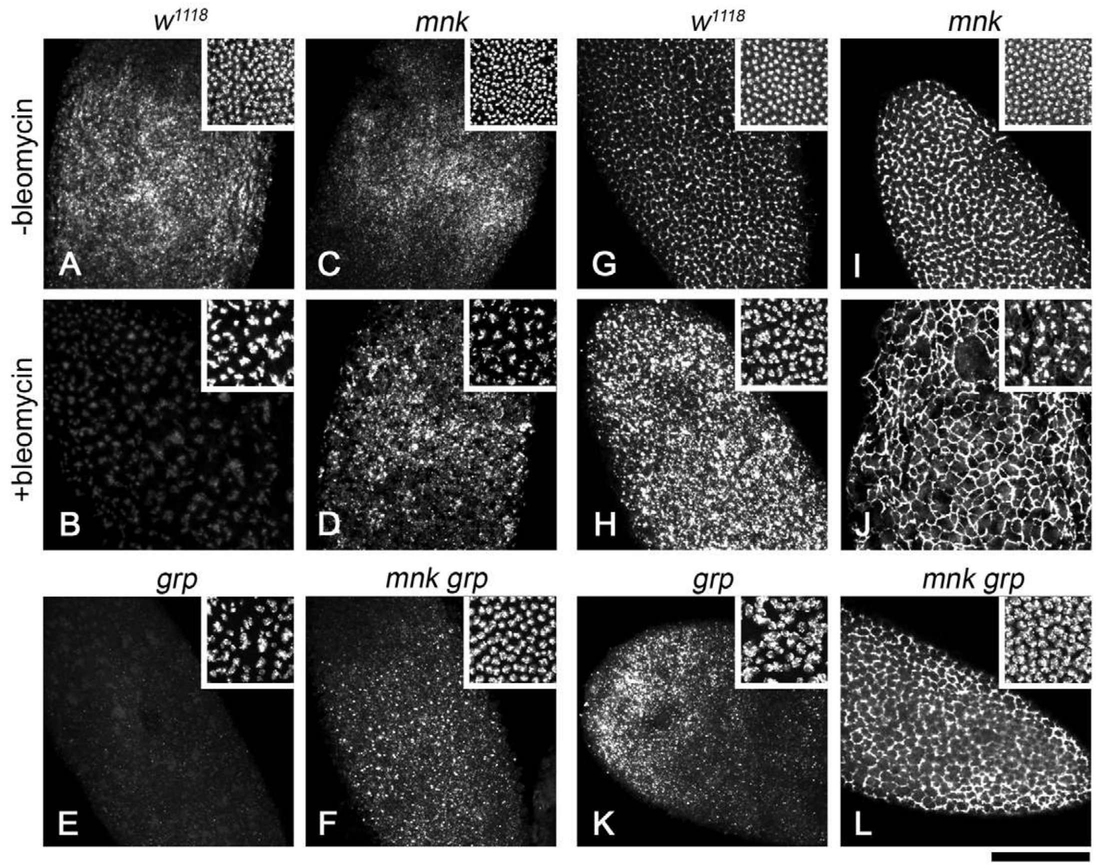

Fig. 5. DNA damage triggers a Chk2-dependent block in the expression of a subset of zygotic genes. Enhanced fluorescence in situ hybridization for *runt* (**A-F**) and *slam* (**G-L**) during early interphase 14 is shown. Embryo stage was judged by blastoderm nuclear density (insets) and DIC images (not shown). (A,C) In w^{1118} and *mnk* mutant embryos, *runt* mRNA is distributed broadly over the central region of the embryo (Klingler and Gergen, 1993). (G,I) *slam* mRNA localizes to the invaginating membrane front, similar to the Slam protein localization reported previously (Lecuit et al., 2002), resulting in a hexagonal network structure around each nucleus. (B) In w^{1118} embryos treated with bleomycin, *runt* transcript is not detectable. (D) By contrast, similarly treated *mnk* mutant embryos express *runt* at the same levels as the embryos without DNA damage. Following bleomycin treatment, *slam* is expressed in both w^{1118} and *mnk* mutant embryos, although *slam* transcript localization is disrupted. This transcript is dispersed in w^{1118} embryos (H) and localizes around the large aneuploid nuclei in *mnk* embryos (J). *runt* expression is also blocked in *grp* mutant embryos, and expression is restored in *mnk grp* double mutants (E,F). By contrast, *slam* transcripts are detected in both *grp* single-mutant and *mnk grp* double-mutant embryos (K,L). DNA damage during the syncytial blastoderm stage and the *grp* mutation thus produce similar gene-specific expression defects. Scale bar: 100 μm.

and developmental defects associated with *grp* mutations, by contrast, are a secondary consequence of DNA-damage signaling via Chk2.

To test more directly the hypothesis that the *grp* mutation leads to DNA damage, we labeled *grp* mutant embryos for phospho-histone H2Av (γH2Av), a homolog of γH2AX that associates with DNA double-strand breaks (Madigan et al., 2002; Rogakou et al., 1999). As shown in Fig. 3, *grp* mutant embryos accumulate γH2Av foci (Fig. 3A-F). These findings are consistent with earlier observations indicating that *grp* mutant embryos accumulate DNA lesions (Fogarty et al., 1997). In a variety of organisms, Chk2 is activated via phosphorylation by Atm or Atr, which leads to oligomerization and auto-phosphorylation. The active phosphorylated form of Chk2 shows reduced electrophoretic mobility by SDS-PAGE (Bartek et al., 2001; Brodsky et al., 2004). In *grp* mutants, Chk2 showed a modest shift, consistent with kinase activation (Fig. 3G). Mutations in *grp* thus lead to both DNA damage and Chk2 phosphorylation, and the MBT block in *grp* mutants is efficiently suppressed by the *mnk* mutation. DNA-damage signaling via Chk2 thus appears to induce developmental arrest in *grp* mutants.

DNA damage induces a Chk2-dependent block to blastoderm cellularization

To determine whether DNA damage and Chk2 activation are sufficient to block developmental progression, we assayed cellularization in wild-type and *mnk* mutant embryos injected with DNA-damaging agents after the final syncytial blastoderm division. For the majority of these studies, embryos were injected with bleomycin, a radiomimetic drug that produces DNA double-strand breaks, and cellularization was followed by time-lapse microscopy (Fig. 4). Bleomycin injection during the final syncytial mitosis (mitosis 13) or during early interphase 14 blocked cellularization in 9 out of the 11 wild-type embryos examined (Fig. 4A-D, and see Movie 5 in the supplementary material). By contrast, 9 out of 9 *mnk* mutant embryos injected during mitosis 13 or interphase 14 cellularized normally (Fig. 4E-H, and see Movie 6 in the supplementary material). Interestingly, these embryos did not subsequently gastrulate. In addition, wild-type embryos injected with DNA-damaging agents after initiating membrane invagination went on to complete cellularization, but these embryos also failed to gastrulate (data not shown). DNA damage early in interphase 14 thus triggers a Chk2-dependent block to cellularization. DNA damage during cellularization, by contrast, induces a Chk2-independent block to gastrulation.

To determine the effect of DNA damage on transcriptional activation at the MBT, we analyzed expression of two early zygotic genes, *slam* and *runt*, in wild-type (w^{1118}) and *mnk* mutant embryos treated with bleomycin. Previous studies have shown that X-ray treatment blocks zygotic *runt* transcription during interphase 14 (Brodsky et al., 2000), and we found that all of the bleomycin-treated wild-type embryos that showed clear cytological indications of DNA damage failed to express *runt* (Fig. 5B). Following bleomycin treatment, a subset of cytologically normal cellular blastoderm-stage embryos were present, and these embryos expressed *runt* at high levels in the normal seven-stripe pattern (see Fig. S3 in the supplementary material). Because bleomycin injection early in interphase 14 consistently blocked cellularization, the embryos that expressed *runt* in a seven-stripe pattern appear to have initiated cellularization when drug treatment was started, or were not efficiently permeablized and thus did not receive a sufficient dose of inhibitor. Bleomycin-treated *mnk* mutant embryos consistently expressed *runt* at levels comparable to untreated wild-type and *mnk* controls (Fig. 5C,D). Damage-dependent Chk2 activation thus appears to block *runt* transcription. We did detect *slam* transcript in wild-type embryos treated with bleomycin, but transcript localization was severely disrupted (Fig. 5H). In bleomycin-treated *mnk* mutants, *slam* expression and distribution were similar to untreated controls (Fig. 5J). Very similar Chk2-dependent defects are observed in *grp* mutants (Fig. 5E,F,K,L). DNA-damage signaling via Chk2 thus disrupts transcript localization and transcriptional activation of a subset of zygotic genes, and activation of this pathway appears to induce the transcription defects associated with replication-checkpoint mutations.

DISCUSSION

Studies in lower eukaryotes initially defined checkpoints as non-essential pathways that delay cell cycle progression in response to external stress (Hartwell and Weinert, 1989). Subsequently, checkpoint mutations in higher eukaryotes were found to induce developmental defects and embryonic lethality (Conn et al., 2004; Kalogeropoulos et al., 2004; Liu et al., 2000; Takai et al., 2000; Petrus et al., 2004; Shimuta et al., 2002). In *Drosophila*, the DNA-replication checkpoint is required to delay the cell cycle during the late cleavage stage, and checkpoint mutants subsequently fail to cellularize or activate zygotic gene expression at the MBT (Sibon et al., 1999; Sibon et al., 1997). These findings suggested that the replication checkpoint has a direct role in metazoan developmental. Alternatively, the observed developmental defects could be an indirect consequence of checkpoint failure.

Here, we show that a null mutation in *mnk*, which encodes the conserved DNA-damage signaling kinase Chk2, efficiently suppresses the cellularization and zygotic gene-activation defects in *grp*, but does not restore wild-type cell cycle timing or replication-checkpoint function. We therefore conclude that progression through the *Drosophila* MBT does not directly require Chk1 or checkpoint-dependent cell cycle delays. Instead, our data indicate that the essential function for the replication checkpoint is to prevent DNA damage during the syncytial blastoderm divisions, which triggers a Chk2-dependent block to zygotic gene activation and cellularization. Supporting this proposal, DNA-damaging agents trigger a Chk2-dependent block to cellularization and zygotic gene activation, and *grp* mutations accumulate DNA double-strand breaks. Chk2 is likely to have multiple targets during this developmental response to DNA damage; these targets may include transcription factors that control the expression of genes implicated in cell cycle control and cellularization (Grosshans et al., 2003; Postner and Wieschaus, 1994; Schejter and Wieschaus, 1993; Wieschaus and Sweeton, 1988).

Embryos mutant for *grp* or *mei-41* lack a functional replication checkpoint and progress into mitosis prior to S-phase completion, triggering defects in γ-Tubulin localization and microtubule nucleation (Sibon et al., 2000). These mitotic defects are suppressed by *mnk*, raising the possibility that *mnk* suppresses the *grp* mutant developmental block at the MBT by restoring mitotic function. However, *mnk* does not suppress the chromosome-segregation defects associated with *grp* mutants (Takada et al., 2003). More significantly, inducing DNA damage following the final syncytial blastoderm division triggers a Chk2-dependent block to cellularization. DNA damage can therefore induce a Chk2-dependent developmental block that is distinct from the damage and Chk2-dependent block to mitosis.

The studies outlined here support a simple model in which the developmental arrest associated with *grp* mutations results from defects in the established function for this kinase in cell cycle control. The early cleavage-stage divisions have a simplified S-phase/M-phase cell cycle, and we propose that the crucial function of Chk1 is to delay mitosis until DNA replication is complete. In *grp* mutants, progression into mitosis before replication is complete leads to DNA damage, which activates a Chk2-dependent block to developmental progression. Intriguingly, disrupting Chk1 function also leads to early embryonic lethality in frogs, mice and worms (Conn et al., 2004; Kalogeropoulos et al., 2004; Liu et al., 2000; Takai et al., 2000; Kalogeropoulos et al., 2004; Petrus et al., 2004; Shimuta et al., 2002). Chk1 knockdown in *Xenopus* and *Chk1* (also known as *Chek1* – Mouse Genome Informatics) mutations in mouse lead to apoptotic death of the embryo, consistent with a DNA-damage response (Takai et al., 2000; Carter and Sible, 2003; Shimuta et al., 2002). We therefore speculate that Chk1 has a conserved function in maintaining genome integrity during the cleavage stage, and that the early embryonic lethality in checkpoint mutants is a consequence of DNA-damage signaling.

We would like to thank P. Gergen and M. Brodsky for providing plasmids and *mnk* fly stocks, respectively; and B. Benoit for critical reading of the manuscript. The α-Spectrin monoclonal antibody developed by D. Branton and R. Dubreuil was obtained from the Developmental Studies Hybridoma Bank at the University of Iowa, Department of Biological Sciences, Iowa City, IA 52242. This work was supported by a grant to W.E.T. from the National Institute of General Medical Sciences, National Institutes of Health (RO1 GM50898).

Supplementary material

Supplementary material for this article is available at http://dev.biologists.org/cgi/content/full/134/9/1737/DC1

References

Bartek, J., Falck, J. and Lukas, J. (2001). CHK2 kinase–a busy messenger. *Nat. Rev. Mol. Cell Biol.* **2**, 877-886.

Bashirullah, A., Halsell, S. R., Cooperstock, R. L., Kloc, M., Karaiskakis, A., Fisher, W. W., Fu, W., Hamilton, J. K., Etkin, L. D. and Lipshitz, H. D. (1999). Joint action of two RNA degradation pathways controls the timing of maternal transcript elimination at the midblastula transition in Drosophila melanogaster. *EMBO J.* **18**, 2610-2620.

Brodsky, M. H., Sekelsky, J. J., Tsang, G., Hawley, R. S. and Rubin, G. M. (2000). mus304 encodes a novel DNA damage checkpoint protein required during Drosophila development. *Genes Dev.* **14**, 666-678.

Brodsky, M. H., Weinert, B. T., Tsang, G., Rong, Y. S., McGinnis, N. M., Golic,

K. G., Rio, D. C. and Rubin, G. M. (2004). Drosophila melanogaster MNK/Chk2 and p53 regulate multiple DNA repair and apoptotic pathways following DNA damage. *Mol. Cell. Biol.* **24**, 1219-1231.

Carter, A. D. and Sible, J. C. (2003). Loss of XChk1 function triggers apoptosis after the midblastula transition in Xenopus laevis embryos. *Mech. Dev.* **120**, 315-323.

Cha, B. J., Koppetsch, B. S. and Theurkauf, W. E. (2001). In vivo analysis of Drosophila bicoid mRNA localization reveals a novel microtubule-dependent axis specification pathway. *Cell* **106**, 35-46.

Conn, C. W., Lewellyn, A. L. and Maller, J. L. (2004). The DNA damage checkpoint in embryonic cell cycles is dependent on the DNA-to-cytoplasmic ratio. *Dev. Cell* **7**, 275-281.

Edgar, B. A. and Datar, S. A. (1996). Zygotic degradation of two maternal Cdc25 mRNAs terminates Drosophila's early cell cycle program. *Genes Dev.* **10**, 1966-1977.

Edgar, B. A., Kiehle, C. P. and Schubiger, G. (1986). Cell cycle control by the nucleo-cytoplasmic ratio in early Drosophila development. *Cell* **44**, 365-372.

Edgar, B. A., Sprenger, F., Duronio, R. J., Leopold, P. and O'Farrell, P. H. (1994). Distinct molecular mechanism regulate cell cycle timing at successive stages of Drosophila embryogenesis. *Genes Dev.* **8**, 440-452.

Foe, V. E., Odell, G. M. and Edgar, B. A. (1993). Mitosis and morphogenesis in the Drosophila embryo: point and counterpoint. In *The Development of Drosophila melanogaster* (ed. M. Bate and A. Martinez Arias), pp. 149-300. Cold Spring Harbor, NY: Cold Spring Harbor Laboratory Press.

Fogarty, P., Campbell, S. D., Abu-Shumays, R., Phalle, B. S., Yu, K. R., Uy, G. L., Goldberg, M. L. and Sullivan, W. (1997). The Drosophila grapes gene is related to checkpoint gene chk1/rad27 and is required for late syncytial division fidelity. *Curr. Biol.* **7**, 418-426.

Grosshans, J., Muller, H. A. and Wieschaus, E. (2003). Control of cleavage cycles in Drosophila embryos by fruhstart. *Dev. Cell* **5**, 285-294.

Hartley, R. S., Rempel, R. E. and Maller, J. L. (1996). In vivo regulation of the early embryonic cell cycle in Xenopus. *Dev. Biol.* **173**, 408-419.

Hartley, R. S., Sible, J. C., Lewellyn, A. L. and Maller, J. L. (1997). A role for cyclin E/Cdk2 in the timing of the midblastula transition in Xenopus embryos. *Dev. Biol.* **188**, 312-321.

Hartwell, L. H. and Weinert, T. A. (1989). Checkpoints: controls that ensure the order of cell cycle events. *Science* **246**, 629-634.

Kalogeropoulos, N., Christoforou, C., Green, A. J., Gill, S. and Ashcroft, N. R. (2004). chk-1 is an essential gene and is required for an S-M checkpoint during early embryogenesis. *Cell Cycle* **3**, 1196-1200.

Kane, D. A. and Kimmel, C. B. (1993). The zebrafish midblastula transition. *Development* **119**, 447-456.

Klingler, M. and Gergen, J. P. (1993). Regulation of runt transcription by Drosophila segmentation genes. *Mech. Dev.* **43**, 3-19.

Lecuit, T., Samanta, R. and Wieschaus, E. (2002). slam encodes a developmental regulator of polarized membrane growth during cleavage of the Drosophila embryo. *Dev. Cell* **2**, 425-436.

Liu, Q., Guntuku, S., Cui, X. S., Matsuoka, S., Cortez, D., Tamai, K., Luo, G., Carattini-Rivera, S., DeMayo, F., Bradley, A. et al. (2000). Chk1 is an essential kinase that is regulated by Atr and required for the G(2)/M DNA damage checkpoint. *Genes Dev.* **14**, 1448-1459.

Madigan, J. P., Chotkowski, H. L. and Glaser, R. L. (2002). DNA double-strand break-induced phosphorylation of Drosophila histone variant H2Av helps prevent radiation-induced apoptosis. *Nucleic Acids Res.* **30**, 3698-3705.

Masrouha, N., Yang, L., Hijal, S., Larochelle, S. and Suter, B. (2003). The Drosophila chk2 gene loki is essential for embryonic DNA double-strand-break checkpoints induced in S phase or G2. *Genetics* **163**, 973-982.

Newport, J. and Kirschner, M. (1982). A major developmental transition in early Xenopus embryos: II. Control of the onset of transcription. *Cell* **30**, 687-696.

O'Farrell, P. H., Stumpff, J. and Su, T. T. (2004). Embryonic cleavage cycles: how is a mouse like a fly? *Curr. Biol.* **14**, R35-R45.

Peters, M., DeLuca, C., Hirao, A., Stambolic, V., Potter, J., Zhou, L., Liepa, J., Snow, B., Arya, S., Wong, J. et al. (2002). Chk2 regulates irradiation-induced, p53-mediated apoptosis in Drosophila. *Proc. Natl. Acad. Sci. USA* **99**, 11305-11310.

Petrus, M. J., Wilhelm, D. E., Murakami, M., Kappas, N. C., Carter, A. D., Wroble, B. N. and Sible, J. C. (2004). Altered expression of Chk1 disrupts cell cycle remodeling at the midblastula transition in Xenopus laevis embryos. *Cell Cycle* **3**, 212-217.

Postner, M. A. and Wieschaus, E. F. (1994). The nullo protein is a component of the actin-myosin network that mediates cellularization in Drosophila melanogaster embryos. *J. Cell Sci.* **107**, 1863-1873.

Rogakou, E. P., Boon, C., Redon, C. and Bonner, W. M. (1999). Megabase chromatin domains involved in DNA double-strand breaks in vivo. *J. Cell Biol.* **146**, 905-916.

Schejter, E. D. and Wieschaus, E. (1993). bottleneck acts as a regulator of the microfilament network governing cellularization of the Drosophila embryo. *Cell* **75**, 373-385.

Schweisguth, F., Lepesant, J. A. and Vincent, A. (1990). The serendipity alpha gene encodes a membrane-associated protein required for the cellularization of the Drosophila embryo. *Genes Dev.* **4**, 922-931.

Shimuta, K., Nakajo, N., Uto, K., Hayano, Y., Okazaki, K. and Sagata, N. (2002). Chk1 is activated transiently and targets Cdc25A for degradation at the Xenopus midblastula transition. *EMBO J.* **21**, 3694-3703.

Sibon, O. C., Stevenson, V. A. and Theurkauf, W. E. (1997). DNA-replication checkpoint control at the Drosophila midblastula transition. *Nature* **388**, 93-97.

Sibon, O. C., Laurencon, A., Hawley, R. and Theurkauf, W. E. (1999). The Drosophila ATM homologue Mei-41 has an essential checkpoint function at the midblastula transition. *Curr. Biol.* **9**, 302-312.

Sibon, O. C., Kelkar, A., Lemstra, W. and Theurkauf, W. E. (2000). DNA-replication/DNA-damage-dependent centrosome inactivation in Drosophila embryos. *Nat. Cell Biol.* **2**, 90-95.

Su, T. T., Campbell, S. D. and O'Farrell, P. H. (1999). Drosophila grapes/CHK1 mutants are defective in cyclin proteolysis and coordination of mitotic events. *Curr. Biol.* **9**, 919-922.

Takada, S., Kelkar, A. and Theurkauf, W. E. (2003). Drosophila checkpoint kinase 2 couples centrosome function and spindle assembly to genomic integrity. *Cell* **113**, 87-99.

Takai, H., Tominaga, K., Motoyama, N., Minamishima, Y. A., Nagahama, H., Tsukiyama, T., Ikeda, K., Nakayama, K., Nakanishi, M. and Nakayama, K. (2000). Aberrant cell cycle checkpoint function and early embryonic death in Chk1(–/–) mice. *Genes Dev.* **14**, 1439-1447.

Tautz, D. and Pfeifle, C. (1989). A non-radioactive in situ hybridization method for the localization of specific RNAs in Drosophila embryos reveals translational control of the segmentation gene hunchback. *Chromosoma* **98**, 81-85.

Theurkauf, W. E. (1994). Immunofluorescence analysis of the cytoskeleton during oogenesis and early embryogenesis. *Methods Cell Biol.* **44**, 489-505.

Tsai, C. and Gergen, P. (1995). Pair-rule expression of the Drosophila fushi tarazu gene: a nuclear receptor response element mediates the opposing regulatory effects of runt and hairy. *Development* **121**, 453-462.

Walworth, N. C. (2001). DNA damage: Chk1 and Cdc25, more than meets the eye. *Curr. Opin. Genet. Dev.* **11**, 78-82.

Wieschaus, E. and Sweeton, D. (1988). Requirements for X-linked zygotic gene activity during cellularization of early Drosophila embryos. *Development* **104**, 483-493.